Electron–Nuclear Double Resonance Studies of Oxidized *Escherichia coli* Sulfite Reductase: ^{1}H, ^{14}N, and ^{57}Fe Measurements†

John F. Cline,‡ Peter A. Janick,§ Lewis M. Siegel,*,§ and Brian M. Hoffman*,‡

Department of Chemistry, Northwestern University, Evanston, Illinois 60201, and Department of Biochemistry, Duke University Medical Center, and Veterans Administration Hospital, Durham, North Carolina 27705

Received May 13, 1985; Revised Manuscript Received July 31, 1985

ABSTRACT: We have employed electron–nuclear double resonance (ENDOR) spectroscopy to study the bridged siroheme–$[Fe_4S_4]$ cluster that forms the catalytically active center of the oxidized hemoprotein subunit (SiR^o) of *Escherichia coli* NADPH–sulfite reductase. The siroheme ^{57}Fe hyperfine coupling (A_z = 27.6 MHz, A_y = 26.8 MHz) is similar to that of other high-spin heme systems ($A \approx 27$ MHz). Bonding parameters obtained from the ^{14}N hyperfine coupling constants of the siroheme pyrrole nitrogens are consistent with a model of a nonplanar π system of reduced aromaticity. The absence of hyperfine coupling to the ^{14}N of an axial ligand, such as is observed for the histidine ^{14}N of metmyoglobin (A_z = 11.55 MHz), rules out the possibility that imidazolate acts as the bridge between the siroheme and the $[Fe_4S_4]$ cluster. Proton ENDOR of the deuterium-exchanged protein indicates that H_2O does not function as a sixth axial ligand and suggests that the ferrisiroheme is five-coordinate. ^{57}Fe ENDOR measurements confirm the results of Mössbauer spectroscopy for the $[Fe_4S_4]$ cluster. They also disclose a slight anisotropy of the cluster ^{57}Fe coupling that may be associated with the mechanism by which the siroheme and cluster spins are coupled.

Escherichia coli sulfite reductase catalyzes the six-electron reduction of sulfite to sulfide (Siegel et al., 1982). Its monomeric hemoprotein subunit, M_r = 54000 (Siegel & Davis, 1974), contains a bridged siroheme–$[Fe_4S_4]$ cluster as its catalytically active center (Christner et al., 1981). This multimetallic center represents the site of sulfite binding and its multielectron reduction. A number of optical, EPR,[1] and Mössbauer spectroscopic studies on sulfite reductase in various states of oxidation–reduction and ligation have been reported by Siegel, Münck, and their co-workers (Christner et al., 1981, 1983a,b, 1984; Siegel et al., 1982; Janick & Siegel, 1982, 1983; Janick et al., 1983). These studies have shown that the heme Fe is in the high-spin Fe(III) state in the oxidized enzyme as isolated, while the $[Fe_4S_4]$ cluster is in the +2 (oxidized ferredoxin) state. The heme Fe is magnetically exchange-coupled to one of the Fe atoms of the cluster, presumably through a covalently linked bridging ligand. The coupling is not broken by applied magnetic fields of up to 60 T and is present in all oxidation states of the enzyme and in all enzyme complexes with exogenously added ligands examined. The strength of the coupling is not known for the oxidized enzyme; however, it has been estimated recently (Christner et al., 1984) to be $|J| = 1\text{–}3$ cm^{-1} in the two-electron-reduced enzyme and $|J| > 6$ cm^{-1} in the one-electron-reduced enzyme–S^{2-} complex.

We have initiated a series of ENDOR investigations on the *E. coli* sulfite reductase hemoprotein subunit (SiR-HP) with the object of determining the state of ligation of the siroheme Fe in various enzyme complexes, with particular emphasis on the nature of the ligand that bridges the heme and $[Fe_4S_4]$ centers. ENDOR can also yield information on the anisotropy of the coupling between the heme and $[Fe_4S_4]$ cluster Fe atoms, as well as the g and A tensors of the cluster and heme irons and of the pyrrole nitrogens coordinating the heme iron. Since siroheme is the first example of an enzymatically functional isobacteriochlorin (i.e., a tetrahydroporphyrin with adjacent pyrrole rings reduced; Siegel et al., 1973; Murphy et al., 1973; Scott et al., 1978), this type of information is of basic significance for our understanding of the role of ring oxidation state in heme-based catalysis. In this paper we report the ENDOR spectroscopy of the oxidized enzyme, SiR^o. The results indicate that imidazolate does not act as the bridge between the siroheme and the $[Fe_4S_4]$ cluster and that in this enzyme state the heme Fe(III) is without H_2O as sixth ligand and probably is five-coordinate. We also report information concerning the bonding within the siroheme and to the heme iron and the relative rotation of the siroheme g tensor in SiR^o, as well as the anisotropy of the hyperfine coupling of the $[Fe_4S_4]$ cluster to the system spin of the oxidized enzyme.

Materials and Methods

E. coli NADPH–sulfite reductase (a complex of the hemoprotein subunit with a specific flavoprotein), natural abundance Fe, was purified by the procedure of Siegel et al. (1973). In order to obtain ^{57}Fe-enriched enzyme, *E. coli* K12 cells were grown as previously described (Siegel et al., 1973) with 0.5 mg/L ^{57}Fe (95% enrichment, New England Nuclear), and NADPH–sulfite reductase was purified by the same procedure. With both enzyme samples, the SiR^o hemoprotein subunit was isolated as described by Siegel & Davis (1974). The enzyme was buffered in 50 mM potassium phosphate, pH 7.7, containing 0.1 mM EDTA, and the siroheme concentration was determined optically by using an $E_{591} = 1.8 \times 10^4$ M^{-1} cm^{-1} (Siegel et al., 1982).

The ENDOR spectrometer is based on a modified Varian E109 EPR spectrometer. Experiments were performed with

† Work at Northwestern University was supported by Grant HL-13531 from the National Institutes of Health. The ENDOR spectrometer was purchased with a grant from the NSF Biological Instrumentation Program (PCM-8116106). Work at Duke University School of Medicine and the Veterans Administration Hospital was supported by Grant GM-32210 from the National Institutes of Health and Project Grant 7875-01 from the Veterans Administration.

‡ Northwestern University.

§ Duke University Medical Center and Veterans Administration Hospital.

[1] Abbreviations: ENDOR, electron–nuclear double resonance; SiR, sulfite reductase; SiR-HP, SiR hemoprotein subunit; SiR^o, oxidized SiR-HP; $[Fe_4S_4]$, tetrairon iron–sulfur center; EPR, electron paramagnetic resonance; EDTA, ethylenediaminetetraacetic acid; TPP, tetraphenylporphyrin.

0006-2960/85/0424-7942$01.50/0

a silvered brass TE_{102} cavity (Roberts, 1982) held at 2.0 K in a Janis Corp. emersion Dewar. The radio frequency (rf) was provided by a Hewlett-Packard (HP) Model 8601A rf generator driven by a linear voltage ramp from a Nicolet Model 1280 computer. The rf power was amplified by Electronic Navigation Instruments (ENI) Model A150 or 3200L 150-W amplifier. Radio-frequency power of 20 W gave ~1 G in the rotating frame. The ENDOR signals were observed as a decrease in the 100-kHz modulated, dispersion-mode EPR signal and accumulated in the computer. All ENDOR patterns were observed with both increasing and decreasing frequency sweeps; parameters reported are the average of these measurements.

ENDOR is performed at a fixed applied field, H_0, and is manifested by changes in the EPR signal intensity that result from nuclear transitions induced by a swept radio-frequency field (Abragam & Bleaney, 1970; Atherton, 1973). For a particular orientation of the external field relative to the principal axes of the g tensor, the first-order ENDOR spectrum of a paramagnet with effective spin $S = {}^1/_2$, interacting with a set of magnetically equivalent ^{14}N nuclei, typically consists of four transitions at frequencies

$$\nu_{\pm}^{N} = A^{N}/2 \pm \nu_{N} \pm 3P^{N}/2 \quad (1)$$

where A is the hyperfine interaction, P is the quadrupole coupling, and ν_N is the nuclear Larmor frequency. Equation 1 describes a four-line pattern centered at the angle-dependent hyperfine frequency $A/2$, assuming $A/2 \gg \nu_N$, P as is true here.

A set of magnetically equivalent protons is expected to give a single pair of ENDOR transitions separated by the angle-dependent hyperfine coupling constant A^H and mirrored about the free-proton Larmor frequency $\nu_H = g_H\beta_n H_0/h$ (14.69 MHz at 3450 G) according to the equation

$$\nu_{\pm}^{H} = \nu_{H} \pm A^{H}/2 \quad (2)$$

The ENDOR pattern of an individual ^{57}Fe nucleus, or a set of magnetically equivalent nuclei, consists of a pair of lines centered at half the hyperfine coupling, $A/2$, and split by twice the nuclear Larmor frequency, ν_{Fe} (ν_{Fe} = 0.14 MHz at 1000 G; ν_{Fe} = 0.47 MHz at 3450 G), as given by

$$\nu_{\pm}^{Fe} = A^{Fe}/2 \pm \nu_{Fe} \quad (3)$$

Because ν_{Fe} is small, at low fields the splitting might not be resolved.

The paramagnetic centers of high-spin ($S = {}^5/_2$) ferri-hemoproteins such as SiR° and metmyoglobin (met-Mb) exhibit EPR signals that can be treated as arising from a paramagnet with effective spin $S' = {}^1/_2$. The hyperfine couplings obtained through eq 1–3 are in the $S' = {}^1/_2$ representation, A', and must be converted to the principal values of the hyperfine Hamiltonian, A_i, for the true $S = {}^5/_2$ spin representation. For a system where the g and A tensors are coaxial, the hyperfine Hamiltonian in the true spin representation is $H = \sum_i S_i A_i I_i$. In the effective spin representation this becomes $H = \sum_i S_i' A_i' I_i$, where $A_i' = (g_i'/g_e)A_i$; g_e is the free-electron g value and g_i' is the ith principal value of the $S' = {}^1/_2$ g tensor. In a system where the g and A tensors are noncoaxial, in the g frame the true spin representation of the hyperfine Hamiltonian becomes $H = \sum_{ij} S_i A_{ij} I_j$. For the effective spin representation ($S' = {}^1/_2$) the hyperfine Hamiltonian is $H = \sum S_i' A_{ij}' I_j$ where $A_{ij}' = (g_i'/g_e)A_{ij}$. Unless explicitly noted, all coupling constants will be quoted in the $S = {}^5/_2$ spin representation.

ENDOR simulations were performed on an Apple II Plus computer (Hoffman et al., 1984, 1985). The program includes hyperfine and quadrupole couplings according to Thomas & Lund (1975). Calculation and interpretation of hyperfine tensor values are discussed in the text. Although EPR and ENDOR line widths were included in the calculations, it was found that the EPR line width contribution was insignificant over a wide range of values.

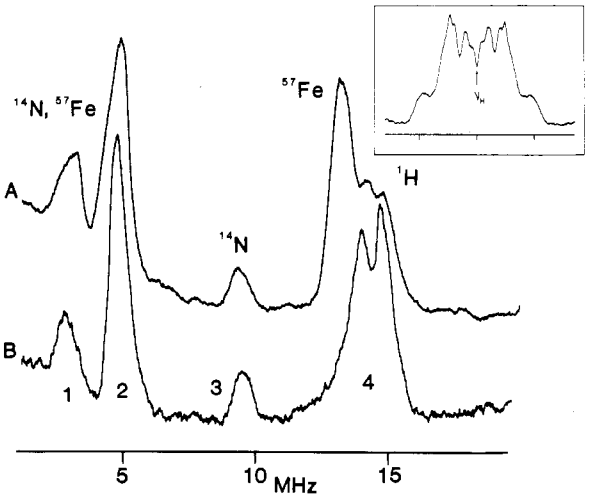

FIGURE 1: Broad-band ENDOR spectra of ^{57}Fe-enriched (A) and ^{56}Fe (B) SiR°, with H_0 set to the high-field edge of the EPR spectrum (g = 1.98). Proton resonances, peak 4; nitrogen resonances, peaks 1–3. In (A) the ^{57}Fe resonances are between peaks 1 and 2 and near peak 4. Conditions: microwave frequency, 9.52 GHz; H_0 = 3450 G; T = 2 K; microwave power, 0.2 mW; 100-kHz field modulation, ~4 G; rf power, 20 W; rf scan rate, 5 MHz/s. Inset: SiR° ^1H ENDOR at g_z'. Six different ^1H doublets are seen split symmetrically within the range of about ±1 MHz (indicated by scale divisions on abscissa) about the proton Larmor frequency (ν_H; the center division). Conditions: H_0 = 3430 G; 100-kHz field modulation, ~0.5 G; rf scan rate, 0.5 MHz/s. Other conditions as in main figure.

RESULTS

ENDOR Assignments. The EPR spectrum associated with the oxidized hemoprotein subunit (SiR°) of *E. coli* NADPH–sulfite reductase is characteristic of a rhombically distorted high-spin ($S = {}^5/_2$) ferriheme, with $g_y' = 6.63$, $g_x' = 5.24$, and $g_z' = 1.98$. When the magnetic field is set to the extreme high-field (g_z') edge of the EPR spectrum of sulfite reductase, the ENDOR signal obtained corresponds to those protein molecules oriented such that the field lies along the heme normal. The broad-band, low-resolution, g_z' ENDOR spectra obtained from ^{57}Fe-enriched and natural abundance protein are presented in parts A and B, respectively, of Figure 1. The feature labeled 4 in Figure 1B is centered at the free-proton Larmor frequency (ν_H); it represents proton ENDOR and is shown at high resolution in the inset. Peaks 1–3 in Figure 1B are associated with ^{14}N, as evidenced by similarity to results for other hemoproteins and by the absence of the partner peaks, at frequencies greater than ν_H, required for proton resonances (eq 2). In the ^{57}Fe-enriched protein, an iron ENDOR feature is clearly visible on the low-frequency side of the proton resonances. In addition, intensity from ^{57}Fe is superposed on ^{14}N peaks 1 and 2 (see below).

Figure 2 presents ENDOR spectra of the ^{57}Fe-enriched (Figure 2A) and natural abundance (Figure 2B) SiR° taken with the magnetic field set near the low-field, g_y', edge of the SiR° EPR spectrum. At the low applied field, the proton resonances come near 5 MHz, and a complicated ^{14}N pattern is located between about 10 and 18 MHz. The ^{14}N ENDOR pattern simplifies somewhat at a true g_y' single-crystal-like orientation (left inset); in this case, the spectra arise from protein molecules oriented such that the field lies along the

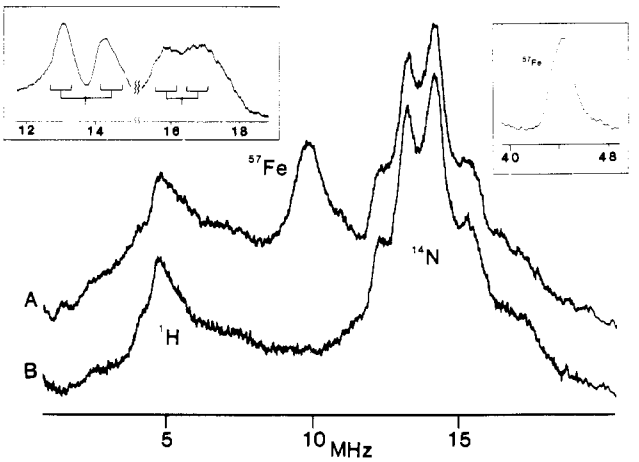

FIGURE 2: Broad-band ENDOR spectra of ^{57}Fe-enriched (A) and ^{56}Fe (B) SiR-HP, with H_0 set near g_y' (g = 6.53). Proton resonances are near 5 MHz and nitrogen resonances near 14 MHz. The ^{57}Fe peaks are near 10 MHz in (A) and 45 MHz (right inset). Conditions: microwave frequency, 9.52 GHz; H_0 = 1050 G. Other conditions as in Figure 1. Left inset: ^{14}N ENDOR spectrum of SiR° with H_0 set to the low-field g_y' edge of the EPR spectrum. Two distinct sets of ^{14}N resonances are seen, one centered below 14 MHz and the other above 16 MHz. The coupling constants ($A_x'/2$) correspond to the center of a set; the resolved quadrupole splittings ($3P$) and the unresolved Larmor splittings ($2\nu_N$) are indicated. Conditions: H_0 = 1000 G; rf scan rate, 10.5 MHz/s. Other conditions as in main figure.

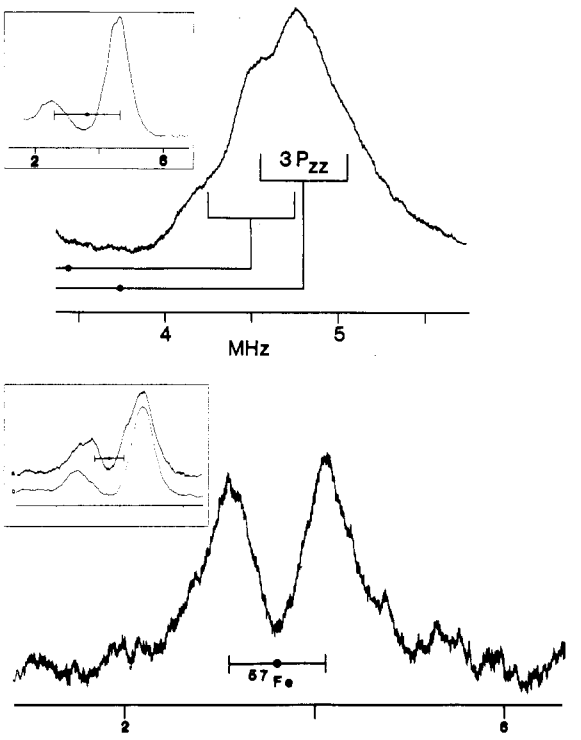

FIGURE 3: Upper panel: ^{14}N ENDOR spectrum at g_z' = 1.98. Inset shows nitrogen ENDOR peaks 1 and 2 of Figure 2; ● indicates an average value of $A^N/2$, and the spread of $2\nu_N$ = 2.12 MHz is displayed. The figure gives an expanded view of peak 2; this represents the high-frequency partners, centered at $A^N/2 + \nu_N$, of the two types of nitrogen resonances. Assignments to individual pairs of coordinating ^{14}N having different values of $A^N/2$ (●) are indicated. The quadrupole splitting ($3P_{zz}$) is indicated. Conditions: H_0 = 3450 G; rf scan rate, 1.25 MHz/s. Other conditions as in Figure 1. Lower panel: ^{57}Fe ENDOR spectrum at g_y' = 1.98 generated by computer subtraction of ^{57}Fe-enriched SiR-HP (upper inset) minus ^{56}Fe SiR-HP (lower inset); scale divisions in inset are the same as in main figure. The difference spectrum is a ^{57}Fe doublet split by $2\nu_{Fe}$, with the coupling constant ($A/2$) indicated (●). Conditions: microwave frequency, 9.52 GHz, H_0 = 3450 G; T = 2.0 K; microwave power, 0.2 mW; 100-kHz field modulation, ~4 G; rf power, 20 W; rf scan rate, 5 MHz/s.

g_y' axis, roughly in the plane of the heme. In addition to ^{1}H and ^{14}N peaks, there are two well-resolved ^{57}Fe resonances seen near g_y', one being at about 9 MHz (Figure 9A) and the other at very high frequency, about 46 MHz (Figure 2, right inset).

Siroheme Nitrogen. When H_0 lies along the heme normal (g_z'), ENDOR spectra taken under low-resolution conditions contain three features, peaks 1–3, that arise from the siroheme pyrrole nitrogens (Figure 1). Features 1 and 2 (Figure 3, upper panel) are separated by $2\nu_N$, which confirms their identification as ^{14}N resonances. This pair of lines is similar to the ^{14}N pattern from the four pyrrole nitrogens of cytochrome P_{450} (LoBrutto et al., 1980), and the average frequency of these two peaks corresponds to a value of $A^N/2$ similar to that for the four heme nitrogens in metmyoglobin (Scholes et al., 1982) and cytochrome P-450. Therefore, lines 1 and 2 are assigned to the superposition of resonances from all four siroheme pyrrole nitrogens, which thus are seen to be chemically similar and to have comparable hyperfine couplings. Expanding peak 2 reveals four features that are reproduced, although with lower resolution, in the partner feature, peak 1 (Figure 3, upper panel). Thus, features 1 and 2 correspond to an eight-line pattern; it can be assigned as the combined result of slight inequivalences between two pairs of equivalent pyrrole nitrogens that exhibit small quadrupole splittings. There are three possible assignments of this pattern, but they give only slightly different hyperfine and quadrupole couplings. The assignment chosen, shown in Figure 3, most closely corresponds to that seen in metmyoglobin (Scholes et al., 1982). The corresponding ^{14}N hyperfine and quadrupole coupling constants along the g_z tensor axis are as follows: A_{1z}' = 7.0 MHz; A_{2z}' = 7.6 MHz; P_z = 0.2 MHz. The difference in coupling between the two pairs of equivalent nitrogens is small (8%), and it is not possible to assign the members of a pair as being either cis or trans with respect to iron.

The frequency of peak 3 is accurately predicted from the hyperfine coupling for the siroheme pyrrole nitrogen through use of the expression

$$\nu = A^N + 2\nu_N$$

appropriate for one of the normally forbidden $\Delta m = \pm 2$ transitions. Thus, peaks 1–3 all are associated with the siroheme. The ^{14}N ENDOR spectra of SiR° thus are noticeable for the absence of peaks associated with an axially coordinated histidine, as are prominently seen in the spectrum of metmyoglobin (Mulks et al., 1979; Scholes et al., 1982).[2] The SiR° spectrum is similar in this regard to that of cytochrome P-450 (LoBrutto et al., 1980), which does not have a histidine or other nitrogenous base as axial ligand. We conclude that the siroheme of SiR does not exhibit a coordinated imidazole and that imidazolate cannot be the link between heme iron and the [Fe_4S_4] cluster.

When the field is set to the low-field edge of the EPR spectrum, ENDOR spectra arise from molecules for which H_0 lies in the heme plane along g_y'. The $\Delta m = \pm 1$ resonances from ^{14}N can be assigned as partially resolved overlapping patterns from two magnetically distinguishable pairs of equivalent ^{14}N, as indicated in Figure 2 (left inset). The center

[2] The $\Delta m = \pm 2$ transition (peak 3) falls in the region where peaks from histidine are observed and is not present in the spectra reported by Scholes and his co-workers. We have confirmed its assignment to pyrrole nitrogen by reexamining metmyoglobin in our spectrometer: both pyrrole $\Delta m = \pm 2$ *and* histidine peaks are observed. The two sets of results presumably differ because the rf field at the sample in our cavity has components that are not perpendicular to H_0.

Table I: ^{14}N Tensor Values (MHz)[a] and ϕ Values (deg)

	A_1	A_2	A_3	P_1	P_2	P_3	ϕ[b]
sulfite reductase							
siroheme	10.6	7.4	7.4	−0.8	1.0	−0.2	30
metmyoglobin[c]							
ferriheme	9.86	6.89	7.11	−0.77	1.04	−0.27	30
histidine	8.33	8.08	11.55	0.31	0.81	−1.12	

[a] Hyperfine tensor components in $S = {}^5/_2$ representation: A_1 corresponds to the M–N direction; A_3 corresponds to the normal to the porphyrin plane. $hP_i = eQq_i/2I(2I-1) = eQq_i/2$ ($I = 1$). [b] Angle by which g tensor is rotated about heme normal away from the x,y axes defined by the N–M–N directions (see text). [c] Scholes et al., 1982.

of gravity of a pattern corresponds to half of the ($S' = {}^1/_2$ representation) ^{14}N hyperfine coupling. Quadrupole splittings are indicated; the splitting due to the nuclear Zeeman interaction ($2\nu_N = 0.62$ MHz) cannot be resolved. This spectrum shows that the four nitrogens that are roughly equivalent chemically, as seen in spectra at g_z', are magnetically inequivalent in pairs when the field is in the heme plane, along g_y'. The ^{14}N hyperfine and quadrupole coupling constants along the g_y' tensor axis are as follows: $A_{1y}' = 32.7$ MHz, $P_{1y} = 0.3$ MHz; $A_{2y}' = 27.5$ MHz, $P_{2y} = 0.5$ MHz.

The major source of the inequivalence among the pyrrole nitrogens is not chemical. As shown in studies of CuTPP (Brown & Hoffman, 1980) and metmyoglobin (Scholes et al., 1982), the hyperfine nitrogen coupling tensor of a pyrrole nitrogen coordinated either to Cu^{2+} or to Fe^{3+} is approximately of axial symmetry, with the unique tensor element corresponding to the M–N direction. Thus, the pyrrole nitrogens, even if chemically identical, would be magnetically distinguishable for a general orientation of the external field, separating into two pairs of trans (inversion-related) nitrogens. In particular, if the external field lies in the N_4 plane at an angle ω with respect to the Fe–N bonds of one pair, it will be at an angle of $90° - \omega$ to those of the other, and the resonance frequencies for the two pairs will differ. By analyzing ENDOR spectra taken at numerous field strengths through use of our recent theory of polycrystalline ENDOR (Hoffman et al., 1984, 1985), we have been able to assign the principal values of the pyrrole nitrogen hyperfine tensors and to determine the relative orientation of the g and hyperfine tensors. In the analysis we consider an idealized coordination geometry in which the pyrrole nitrogens are equivalent and form a square, coplanar with iron. This ignores the small differences among the pyrrole nitrogens of SiR°, as seen in the spectra taken at g_z'. These differences are similar to those seen in met-Mb and have observable influences on spectra at intermediate g values. However, the consequences of the approximations made in this idealization are not significant for our purposes. The ENDOR results for met-Mb further show we may take the ^{14}N tensor to be of axial symmetry with $A_\parallel$ along the M–N bond and may take the P tensor and A tensor to be coaxial.

As a consequence of these simplifications, $A_\perp^N = A_z^N$, the value measured with H_0 set to the g_z single-crystal value. Also, the relative orientation of the g and A^N tensor is determined by a single angle, ϕ, by which the g tensor is rotated with respect to the molecular frame defined by the two, perpendicular, N–M–N directions:

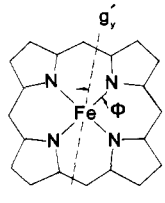

As a final consequence, $P_3 = P_z$, the value measured with H_0 set to the g_z' single-crystal value. Since the quadrupole tensor is traceless (Abragam & Bleaney, 1970), $P_1 + P_2 + P_3 = 0$; therefore, $P_1 + P_2 = -P_3 = -P_z$. These considerations leave three additional parameters to be derived from the experimental spectra taken at g_y' and other magnetic fields away from g_z': $A_\parallel^N$, ϕ, and a single quadrupole tensor parameter. The hyperfine and quadrupole parameters resulting from this analysis of these spectra are listed in Table I. Note that the assignments in Figure 2 are not uniquely determined by that spectrum and the correct assignment is only derived by requiring a consistent interpretation at all fields. As a control for this procedure, an analysis of ENDOR spectra of a frozen solution of metmyoglobin yielded results in good agreement with single-crystal A tensors and rotation angle (see Table I).

The ^{14}N hyperfine tensor of a pyrrole nitrogen characterizes the orbital that is involved in σ-coordination to the ferric ion. The donor orbital may be written as an sp^n hybrid, $\phi_N = f_s\phi_{2p}^N + f_p\phi_{2p}^N$, in which the hybridization is given by the ratio of coefficients squared, $n = f_p^2/f_s^2$; the values of f_s^2 and f_p^2 are obtained respectively from the trace and the anisotropic, or dipolar, parts of hyperfine tensor by standard means.[3] Such calculations give nitrogen hybridizations of 2.0 for CuTPP (Brown & Hoffman, 1980), 2.1 for met-Mb (Scholes et al., 1982), and 2.5 for SiR°, where the small differences among pyrrole nitrogens in met-Mb and observed at g_z' for SiR° have been ignored.

The nitrogens of SiR° thus appear to be somewhat more amine or sp^3-like than imine or sp^2-like than those found in CuTPP and met-Mb. While we recognize the limitations of these calculations, the increased p character in the nitrogens of SiR°, compared to those of met-Mb, is consistent with the idea of reduced aromaticity of the tetrahydroporphyrin ring system of the siroheme and/or deviations from planarity of the ring, as has been found in reduced porphyrin model compounds (Ulman et al., 1980). On the other hand, within the broad experimental uncertainty, the total contribution of the pyrrole nitrogens to the wavefunction is similar in met-Mb and in SiR°, consistent with the results from ^{57}Fe ENDOR (vide infra).

The in-plane principal axes of the g tensor of SiR° are found to lie almost between the nitrogen atoms; the rotation about the N–N diagonal has a value of $\phi \sim 30°$. Since an unconstrained ferrisiroheme having a symmetric axial ligand (e.g., chloroferrisiroheme) has an axially symmetric g tensor (Tang et al., 1976), the rhombicity of the SiR° g tensor and the orientation of the tensor axes presumably reflect asymmetry in the axial ligation.

Proton ENDOR. Figure 1 (inset) presents an expanded proton ENDOR spectrum. It was taken under conditions that

[3] The analysis is similar to that used for CuTPP (Brown & Hoffman, 1980) and repeated for myoglobin (Scholes et al., 1982). The reader is referred to the former paper for the full equations. The simplified forms of the latter were employed here, after correcting errors in eq 5a, 7, and 8.

Table II: ^1H Hyperfine Values (MHz) at g_y'

sulfite reductase	aquometmyoglobin[a]
b	6.02[b]
1.88[c]	~2[c]
d	1.33[d]
1.17	
0.95[e]	0.79[e]
0.78	
	~0.52[e]
	~0.43[f]
0.37	~0.31[f]
0.17	~0.21[f]

[a] Values and assignments taken from Mulks et al. (1979). [b] Assigned to an exchangeable H_2O ligand; none is observed for SiR°. [c] Tentatively assigned to the β-CH proton of the proximal histidine; by analogy, the SiR° resonance may be assigned to the β-CH of the proximal ligand, which is not histidine. [d] Assigned to an exchangeable proton on the δ nitrogen of the proximal histidine. Note the absence in SiR°. [e] Assigned to meso protons; by symmetry at least three different meso protons are expected in SiR. [f] Values are estimated.

permit the resolution of six pairs of features symmetrically distributed about the proton Larmor frequency (ν_H) and associated with individual protons. Table II lists the proton hyperfine coupling constants determined from eq 2 for sulfite reductase, along with the values for aquometmyoglobin. The resolved peaks in the spectrum are unchanged when the protein is dissolved in a D_2O buffer,[4] and thus none of the associated protons are exchangeable.

Some tentative assignments of the sulfite reductase proton couplings may be made by analogy. In met-Mb, a coupling of 0.79 MHz is assigned to the meso protons (Mulks et al., 1979). A siroheme having idealized symmetry would exhibit three distinct types of meso protons and therefore as many as three meso-proton couplings. In the proton ENDOR of sulfite reductase, there are three couplings, of approximately 0.79 MHz, that may be assigned to the meso protons: 1.17, 0.95, and 0.78 MHz. The met-Mb coupling of ~2 MHz has been assigned tentatively to the β-CH proton of the proximal histidine. The ^{14}N ENDOR results rule out histidine as an endogenous axial ligand in SiR°, but the observed coupling of 1.88 MHz also is perfectly appropriate for the β-CH of a cysteinyl residue acting as the bridge between heme iron and cluster. The couplings of 0.37 and 0.17 MHz in SiR° are unassigned but are similar to peaks in myoglobin.

Proton ENDOR measurements can be used to infer the state of the sixth coordination site of the ferrisiroheme of SiR°. In met-Mb, an exchangeable H_2O functions as the sixth ligand, and its protons exhibit a hyperfine coupling of 6.02 MHz that is dipolar (depending only on the Fe–H distance and orientation) in origin. The absence of exchangeable protons in SiR°, or indeed of any proton coupling that is within a factor of 3 of this magnitude, rules out the presence of an H_2O ligand on the siroheme of SiR°. The similarity of the magnetic properties of those of five-coordinate model compounds and of cytochrome P-450 further leads us to infer the ferrisiroheme in SiR° to be five-coordinate.

Iron ENDOR. ^{57}Fe-enriched SiR° shows ENDOR signals from two distinct types of iron. ENDOR spectra with the field set to g_z' clearly show ^{57}Fe ENDOR intensity partially overlapping the ^1H resonance (Figure 1). In addition, changes in the ^{14}N pattern show it to be a superposition of ^{14}N and ^{57}Fe; the ^{57}Fe doublet shows up clearly upon computer subtraction (Figure 3, lower panel). The two peaks obey eq 3 and correspond to a coupling of 7.4 MHz. The partner of the higher frequency ^{57}Fe resonance, visible in Figure 1A at 13 MHz, is not well resolved in subtraction (not shown), presumably because of cross-relaxation to the protons. However, from the observed ν_- peak and eq 3 one obtains a coupling of 27.6 MHz.

By comparison with Mössbauer results of Christner et al. (1981) the low- and high-frequency ^{57}Fe resonances may be assigned to the $[Fe_4S_4]$ cluster and the siroheme, respectively. The Mössbauer data on the $[Fe_4S_4]$ cluster indicate two types of iron, sites I and II, with similar A values (6.2 and −6.1 MHz). The low-frequency ^{57}Fe ENDOR resonance corresponds well with this and is thus assigned to all four $[Fe_4S_4]$ cluster irons, thus confirming that the couplings are equal in magnitude to within ±0.05 MHz. Mössbauer data assign a coupling, A = 27 MHz, to the siroheme iron, in excellent agreement with A = 27.6 MHz from ENDOR spectroscopy.

In proteins, such as SiR°, having a large g anisotropies, ENDOR is uniquely capable of characterizing the anisotropy of the ^{57}Fe hyperfine tensors. With the field set near g_y', comparison of spectra from ^{57}Fe-enriched (Figure 2A) and natural abundance (Figure 2B) SiR° shows the occurrence of ^{57}Fe resonances at ~10 and 45 MHz (see right inset, Figure 2); at this magnetic field the Larmor splitting of the ^{57}Fe peak is small (~0.29 MHz) and unresolved. These features correspond, respectively, to $S = {}^5/_2$ couplings of A = 5.8 MHz for the cluster irons and of A = 26.8 MHz for the siroheme iron.

The hyperfine tensor of siroheme iron is nearly isotropic, as seen in other high-spin ferriheme systems (Scholes et al., 1973), and ENDOR and Mössbauer results are in good agreement. The ENDOR measurements further show that the cluster iron couplings are noticeably anisotropic, with the coupling associated with the normal to the siroheme plane (g_z') being 28% greater than that along g_y'. Unfortunately, a full analysis of the cluster hyperfine tensor was precluded because the ^{57}Fe, ^1H, and ^{14}N peaks all overlap at intermediate values of the magnetic field. Note that the sharpness of the g_y' resonance indicates that all four cluster irons have the same absolute value for A_y and the same degree of anisotropy, despite the fact that two iron sites have positive couplings and two negative. We suspect that this anisotropy reflects the mechanism by which the ferrisiroheme induces hyperfine couplings to the cluster irons and not local properties of those iron sites, for work in progress on the reduced states of the protein shows unusually large anisotropies.

Conclusions

We have examined the ^1H, ^{14}N, and ^{57}Fe ENDOR of the oxidized hemoprotein subunit of *E. coli* NAPH–sulfite reductase and compared them to other high-spin heme systems (Scholes et al., 1982, 1973). The hyperfine parameters of the siroheme ^{57}Fe are normal for a high-spin ferriheme. The bonding parameters of the siroheme nitrogens are similar to those reported previously for CuTPP and for the ferriheme of met-Mb, but they are consistent with expectations for a nonplanar π system of reduced aromaticity.

The absence of a strongly coupled exchangeable proton (or protons), such as is seen in aquometmyoglobin, demonstrates that the heme iron of SiR° does not have a water molecule as its sixth ligand and further suggests that the iron of the siroheme of SiR° is five-coordinated. Perhaps most interesting of all, the absence of a large nitrogen coupling, to an axial ligand, such as is observed for the histidine ^{14}N of metmyo-

[4] In this experiment SiR-HP in D_2O buffer was photoreduced over 2 h by using the deazaflavin–EDTA system of Janick & Siegel (1982) and reoxidized with air 33 min later prior to concentration for ENDOR spectroscopy. This procedure ensured that ready exchange between possible endogenous and exogenous aquo ligands could be effected rapidly, since the oxidized enzyme binds ligands much more slowly than the reduced enzyme.

globin, indicates that the endogenous fifth ligand is not a nitrogenous base. This rules out the possibility of an imidazolate bridge between the siroheme and the $[Fe_4S_4]$ cluster.

The ENDOR results for the $[Fe_4S_4]$ cluster confirm the results of Mössbauer spectroscopy. In addition, we have measured an anisotropy of the cluster ^{57}Fe coupling that may be associated with the mechanism by which heme and cluster spins are coupled.

Registry No. N, 7727-37-9; H, 12408-02-5; ^{57}Fe, 14762-69-7; SiR, 9029-35-0; siroheme, 52553-42-1.

REFERENCES

Abragam, A., & Bleaney, B. (1970) *Electron Paramagnetic Resonance of Transition Ions*, Clarendon Press, Oxford.

Atherton, N. M. (1973) *Electron Spin Resonance*, Wiley, New York.

Brown, T. G., & Hoffman, B. M. (1980) *Mol. Phys. 39*, 1073–1109.

Christner, J. A., Münck, E., Janick, P. A., & Siegel, L. M. (1981) *J. Biol. Chem. 256*, 2098–2101.

Christner, J. A., Münck, E., Janick, P. A., & Siegel, L. M. (1983a) *J. Biol. Chem. 258*, 11147–11156.

Christner, J. A., Janick, P. A., Siegel, L. M., & Münck, E. (1983b) *J. Biol. Chem. 258*, 11157–11164.

Christner, J. A., Münck, E., Kent, T. A., Janick, P. A., Salerno, J. C., & Siegel, L. M. (1984) *J. Am. Chem. Soc. 106*, 6786–6794.

Hoffman, B. M., Martinsen, J., & Venters, R. A. (1984) *J. Magn. Reson. 59*, 110–123.

Hoffman, B. M., Venters, R. A., & Martinsen, J. (1985) *J. Magn. Reson. 62*, 537–542.

Janick, P. A., & Siegel, L. M. (1982) *Biochemistry 21*, 3538–3547.

Janick, P. A., & Siegel, L. M. (1983) *Biochemistry 22*, 504–514.

Janick, P. A., Rueger, D. C., Kreuger, R. J., Barber, M. J., & Siegel, L. M. (1983) *Biochemistry 22*, 396–408.

LoBrutto, R., Scholes, C. P., Wagner, G. C., Gunsalus, I. C., & Debrunner, P. G. (1980) *J. Am. Chem. Soc. 102*, 1167–1170.

Mulks, C. F., Scholes, C. P., Dickinson, L. C., & Lapidot, A. (1979) *J. Am. Chem. Soc. 101*, 1645–1654.

Münck, E., Rhodes, H., Orme-Johnson, W. H., Davis, L. C., Brill, W. J., & Shah, V. K. (1975) *Biochim. Biophys. Acta 400*, 32–53.

Murphy, M. J., Siegel, L. M., Kamin, H., & Rosenthal, D. (1973) *J. Biol. Chem. 248*, 2801–2814.

Roberts, J. (1982) Ph.D. Thesis, Northwestern University, Evanston, IL.

Scholes, C. P., Isaacson, R. A., Yonetani, T., & Feher, G. (1973) *Biochim. Biophys. Acta 322*, 457–462.

Scholes, C. P., Lapidot, A., Mascarenhas, R., Inubushi, T., Isaacson, R. A., & Feher, G. (1982) *J. Am. Chem. Soc. 104*, 2724–2735.

Scott, A. I., Irwin, A. J., Siegel, L. M., & Shoolery, J. M. (1978) *J. Am. Chem. Soc. 100*, 7987–7994.

Siegel, L. M., & Davis, P. S. (1974) *J. Biol. Chem. 249*, 1587–1598.

Siegel, L. M., Murphy, M. J., & Kamin, H. (1973) *J. Biol. Chem. 248*, 1587–1598.

Siegel, L. M., Rueger, D. C., Barber, M. J., Kreuger, R. J., Orme-Johnson, N. R., & Orme-Johnson, W. H. (1982) *J. Biol. Chem. 257*, 6343–6350.

Tang, S. C., Koch, S., Papaefthymiou, G. C., Foner, S., Frankel, R. B., Ibers, J. A., & Holm, R. H. (1976) *J. Am. Chem. Soc. 98*, 2414–2434.

Thuomas, K.-A., & Lund, A. (1975) *J. Magn. Reson. 18*, 12–21.

Ulman, A., Gallucci, J., Fisher, D., and Ibers J. A. (1980) *J. Am. Chem. Soc. 102*, 6854–6855.